JOURNAL OF VIROLOGY, Apr. 2007, p. 3563–3573 Vol. 81, No. 7
0022-538X/07/$08.00+0 doi:10.1128/JVI.02494-06

Heparan Sulfate Binding Can Contribute to the Neurovirulence of Neuroadapted and Nonneuroadapted Sindbis Viruses▽

Kate D. Ryman,[1]* Christina L. Gardner,[1] Crystal W. Burke,[1] Kathryn C. Meier,[1] Joseph M. Thompson,[2] and William B. Klimstra[1]

Department of Microbiology and Immunology, Louisiana State University Health Sciences Center, Shreveport, Louisiana 71130-3932,[1] and Department of Microbiology and Immunology, University of North Carolina at Chapel Hill, Chapel Hill, North Carolina 27599-7290[2]

Received 13 November 2006/Accepted 3 January 2007

Cell culture-adapted laboratory strains of Sindbis virus (SB) exhibit efficient initial attachment to cell surface heparan sulfate (HS) receptors. In contrast, non-cell-adapted strains, such as the SB consensus sequence virus TR339, interact weakly with HS and cell surfaces. Regardless of their HS binding phenotype, most SB strains do not cause fatal disease in adult mice, whether inoculated subcutaneously (s.c.) or intracranially (i.c.). However, laboratory strains of SB can be rendered neurovirulent for adult mice by introduction of a glutamine (Gln)-to-histidine (His) mutation at position 55 of the E2 envelope glycoprotein. In the current work, we have determined that E2 His 55-containing viruses require a second-site mutation (Glu to Lys) at E2 position 70 that confers efficient HS binding in order to exhibit virulence for adult mice and that virulence is correlated with very high infectivity for many cell types. Furthermore, introduction of E2 Lys 70 or certain other HS-binding mutations alone also increased morbidity and/or mortality over that of TR339 for older mice inoculated i.c. However, all viruses containing single HS-binding mutations were attenuated in s.c. inoculated suckling mice in comparison with TR339. These results suggest that HS binding may attenuate viral disease that is dependent on high-titer viremia; however, efficient cell attachment through HS binding can increase virulence, presumably through enhancing the replication of SB within specific host tissues such as the brain.

Sindbis virus (SB) strain AR339 is considered the prototypic virus of the *Alphavirus* genus, family *Togaviridae*. This family of mosquito-borne RNA viruses includes several significant human pathogens and potential bioterrorism or biowarfare agents such as Venezuelan and Eastern equine encephalitis viruses (VEEV and EEEV, respectively) (3, 44). Consequently, there has been a resurgence of interest in characterizing the molecular determinants of alphavirus neurovirulence. Due to the relative difficulty and risk of handling the more pathogenic alphaviruses, SB has been used extensively as a model system for the study of the alphavirus replication cycle and the pathogenesis of disease (reviewed in reference 16).

Many laboratory strains descended from SB AR339 initially attach to cells through interaction with heparan sulfate (HS), a negatively charged glycosaminoglycan (GAG) found on the surfaces of most cells (4, 26). This also appears to be the case with cell culture-adapted laboratory strains of other alphaviruses (1, 18, 39). However, in contrast to laboratory strains, virus particles derived from a cDNA clone representing a consensus sequence of SB group viruses (strain TR339) (32) do not attach efficiently to HS or cell surfaces (26). Furthermore, the cell attachment phenotype of TR339 is indistinguishable from that of a virus generated from a cDNA clone of an ancestral SB AR339 preserved prior to adaptation for growth in cultured cells (W. B. Klimstra, D. E. Deming, R. E. Johnston, and K. D. Ryman, unpublished observations). All SB laboratory strains of known sequence differ from the consensus sequence by the acquisition of positive-charge mutations within the E2 attachment glycoprotein. Similarly, positive-charge mutations that confer HS binding are rapidly selected during amplification of TR339 in cultured cells (26). Other wild-type alphaviruses, including VEEV (1) and Ross River virus (18), can also accumulate positive-charge E2 mutations that promote HS binding during in vitro passage.

The results of several studies have indicated that non-HS-binding strains of SB (5, 26), VEEV (1), foot-and-mouth disease virus (19, 34), tick-borne encephalitis virus (31), and classical swine fever virus (19) are more virulent in animal models than their HS-binding counterparts, suggesting that for these viruses, the HS binding phenotype is a tissue culture adaptation that lowers virus fitness in vivo. We and others have hypothesized that attenuation is due to viremia suppression resulting from nonproductive binding of virus to HS structures in vivo (1, 5, 26). In contrast, HS binding has been documented for clinical isolates of the *Herpesviridae* (see, e.g., reference 41) and *Picornaviridae* (see, e.g., reference 14), raising the possibility that interaction between virus attachment proteins and GAGs does have a productive role in the natural history of some viruses.

Regardless of the HS binding phenotype, nonneuroadapted SB strains are avirulent, failing to cause morbidity or mortality in mice more than 2 weeks old, independently of inoculation route or virus dose (15, 36, 40). However, Griffin and coworkers were able to select an SB strain with adult mouse virulence by alternating intracranial (i.c.) passage of their laboratory

* Corresponding author. Mailing address: Department of Microbiology and Immunology, Louisiana State University Health Sciences Center, Shreveport, LA 71130-3932. Phone: (318) 675-6684. Fax: (318) 675-5764. E-mail: kryman@lsuhsc.edu.

▽ Published ahead of print on 10 January 2007.

strain (SV) in neonatal and weanling mice (17). Mortalities caused by this neurovirulent biological isolate, designated "neuroadapted Sindbis virus" (NSV), were associated with severe encephalomyelitis, kyphoscoliosis, and hind limb paralysis (17) and correlated with the induction of apoptosis in neurons, the primary targets of SB infection in the central nervous system (CNS) (28). A mutation from Gln to His at position 55 of the E2 attachment protein was identified as primarily responsible for this phenotype and could confer adult mouse neurovirulence when introduced into a cDNA clone from a non-adult-virulent SV laboratory strain (29, 42). Although the mechanism by which the E2 His 55 mutation increases adult mouse virulence remains unclear, several explanations for this phenotype have been suggested, including (i) increased infectivity for neurons (27), (ii) increased virus RNA replication within infected neurons (8), (iii) increased apoptotic potential in infected fully differentiated neurons (21, 28, 43), and(iv) death of uninfected neurons due to overproduction of excitatory neurotransmitters (33).

In the current studies, we have investigated whether or not HS binding can contribute to virus replication and virulence in vivo by introducing into TR339, either alone or combined with E2 His 55, mutations previously shown to individually confer HS binding. In these experiments, TR339 was used as an "HS-binding-negative background" in which mutations could be examined for their contribution to virulence and HS binding. The results of these experiments indicate that an HS-binding mutation is required for adult mouse virulence of viruses containing E2 His 55 and that this effect may be specific to the Gln-to-Lys mutation at E2 position 70, which is common to several SB laboratory strains. The resultant adult-neurovirulent virus exhibited a dependence on HS binding for infection of BHK cells similar, but not identical, to that conferred by E2 Lys 70 alone and was more infectious than other viruses for cultured cells derived from tissues of mammalian, arthropod, and avian origins. In agreement with a role for HS binding in the neurovirulence of alphaviruses, several viruses with single HS-binding mutations that attenuated virulence from a subcutaneous (s.c.) inoculation were more virulent than TR339 when inoculated directly into the brains of mice. Therefore, we conclude that, in the absence of a requirement for viremia, HS binding can contribute to alphavirus virulence, presumably by increasing replication within individual organs in vivo.

MATERIALS AND METHODS

Cell lines. Baby hamster kidney (BHK-21 [ATCC CCL-10]), L929 murine fibrosarcoma (ATCC CCL-1), DF-1 chicken fibroblast (ATCC CRL-12203), and Vero African green monkey kidney (ATCC CCL-81) cell lines were maintained in alpha minimal essential medium (α-MEM) supplemented with 10% donor calf serum (DCS), 2.9 mg/ml tryptose phosphate, 0.29 mg/ml L-glutamine, 100 U/ml penicillin, and 0.05 mg/ml streptomycin. Neuro-2A murine neuroblastoma cells (ATCC CCL-131) and C6/36 mosquito cells (ATCC CRL-1660) were maintained in α-MEM with 10% fetal bovine serum (FBS), L-glutamine, and 1% nonessential amino acids. All cells other than DF-1 and C6/36 were incubated at 37°C under 5% CO_2. DF-1 cells were incubated at 40°C and C6/36 cells at 29°C. Chinese hamster ovary (CHO K1 [ATCC CCL-61] and CHO pgsA-745 [ATCC CRL-2242]) cells were maintained in Ham's F-12 medium with 10% FBS and antibiotics. XS106 murine dendritic cells (a gift from A. Takashima [46]) were maintained in complete RPMI 1640 (RPMI 1640 medium supplemented with 10% FBS, L-glutamine, 1% nonessential amino acids, 1 mM sodium pyruvate, 20 μg/ml gentamicin, 5 mM HEPES buffer, and 50 μM β-mercaptoethanol) with 0.5 ng/ml murine granulocyte-monocyte colony-stimulating factor and 5% NS47 murine fibroblast-conditioned supernatant (46). NS47 murine fibroblasts were maintained in complete RPMI 1640.

Sindbis viruses. Construction of the AR339 consensus sequence plasmid pTR339 and of plasmids p39-E2R1, p39-E2K70, and p39-E2R114 has been described previously (26). A Glu-to-Lys mutation was introduced into pTR339 at E2 position 181 by megaprimer PCR mutagenesis, using a mutagenic primer (23) to create p39-E2K181 cDNA. A Gln-to-His mutation was similarly introduced into pTR339 at E2 position 55 to generate p39-E2H55. E2 His 55 was combined with E2 Arg 1, E2 Lys 70, E2 Arg 114, or E2 Lys 181 to generate p39-E2R1H55, p39-E2H55K70, p39-E2H55R114, or p39-E2H55K181, respectively, by megaprimer PCR mutagenesis. Infectious viral RNA was generated by in vitro transcription using a Message Machine kit (Ambion) from XhoI-linearized plasmid DNA templates. RNA was electroporated into BHK-21 cells, and virus particles were harvested from the supernatant 18 to 20 h after electroporation, clarified by centrifugation, and stored at −80°C in single-use aliquots. Virus stocks were titered by a standard BHK-21 cell plaque assay, and titers were expressed as PFU per milliliter. An enhanced green fluorescent protein (eGFP)- or firefly luciferase (fLuc)-expressing double-promoter virus comparable to TR339 was already available (p39mcs-3′eGFP or p39mcs-3′fLuc, respectively) (36). StuI-BssHII restriction fragments from p39-E2K70, p39-E2H55, and p39-H55K70 were cloned into p39mcs-3′eGFP or p39mcs-3′fLuc to create virus reporter clones for each mutant.

Sindbis virus replicon particles. Construction of the eGFP- and fLuc-expressing Sindbis virus bipartite helper replicon systems has been described elsewhere (36, 37). Briefly, replicon genome plasmids (p39-REP-eGFP and p39-REP-fLuc) were constructed, encoding TR339 nonstructural protein genes and the eGFP or fLuc gene downstream of the 26S subgenomic promoter in place of the viral structural protein genes. SB replicon particles (SBRPs) were produced by packaging infectious replicon RNA transcripts in viral structural proteins provided in *trans* by helper RNAs expressing the capsid (pCH) or E1/6K/PE2 (pINT) glycoproteins separately (2, 36, 37). For mutant generation, each parental virus plasmid was digested with StuI and BssHII, and fragments were ligated into the similarly digested pINT glycoprotein helper. In vitro-transcribed RNA from pINT or the E2 mutants, pCH, and the replicon genome expressing either eGFP or fLuc were coelectroporated into BHK-21 cells, and SBRPs were harvested 24 h postelectroporation. From each SBRP preparation, 10% was evaluated by serial passage on BHK-21 cells for the presence of cytopathic effect (CPE)-inducing, propagation-competent virus recombinants or contaminants (30). SBRP stocks were considered virus free for experimental purposes if no CPE was evident after three serial amplifications. Titers of SBRPs expressing eGFP were determined by infection of BHK-21 cells and expressed as green infectious units per milliliter. Titers of SBRPs expressing fLuc were determined by a luciferase assay (Promega) of BHK cell lysates infected as described above and are represented as the highest dilution at which luciferase expression could be detected above background.

Mice. Pregnant female mice (13 to 15 days of gestation) and 21-day-old and 5-week-old outbred CD-1 mice were purchased from Charles River Laboratories. Mice were housed in the Animal Resource Center at Louisiana State University Health Sciences Center—Shreveport under specific-pathogen-free conditions. All procedures were carried out in accordance with institutional guidelines for animal care and use.

Mortality studies. Virus inocula were diluted in low-endotoxin phosphate-buffered saline (PBS) supplemented with 1% DCS, calcium, and magnesium (PBS–1% DCS) to contain 1×10^3 PFU of TR339 in a 10-μl volume (i.e., 1×10^5 PFU/ml) and were administered either s.c. in each hind leg footpad or i.c. 39-R1H55, 39-H55, 39-K70, and 39-H55K70 stocks were diluted identically to TR339 to ensure that equal numbers of virus particles were given. For neonatal mice, the virus was diluted similarly to contain 1×10^3 PFU of TR339 in 10 μl of diluent (or equivalent dilutions of other viruses), and the virus was administered s.c. in the axial region. Mock-infected mice received 10 μl of PBS–1% DCS by the same routes. Virus-infected and corresponding mock-infected mice were observed at 12-h intervals, scored for degree of sickness, and weighed daily. Average survival times (AST) and percent mortality were calculated as described by Klimstra et al. (25).

Plaque assays. Each virus was diluted serially to ~100 BHK infectious units per 200 μl in PBS–1% DCS. Cells were infected in 12-well or 60-mm plates for 60 min at 37°C. Depending on the experiment, plates were either washed twice with VB prior to overlay or overlaid directly with a 0.5% immunodiffusion agarose/growth medium solution. After 24 h, plates were stained with neutral red, and plaques were enumerated as PFU per milliliter. BHK cell plaque sizes were quantitated using calipers by measurement of 20 plaques on neutral-red-stained monolayers.

TABLE 1. Genotypes of viruses used in the current studies[a]

Virus	Amino acid at the following position of E2:				
	1	55	70	114	181
TR339	Ser	Gln	Glu	Ser	Glu
39-E2H55	Ser	His	Glu	Ser	Glu
39-E2K70	Ser	Gln	Lys	Ser	Glu
39-E2H55K70	Ser	His	Lys	Ser	Glu
39-E2R1	Arg	Gln	Glu	Ser	Glu
39-E2K181	Ser	Gln	Glu	Ser	Lys
39-E2H55R1	Arg	His	Glu	Ser	Glu
39-E2H55R114	Ser	His	Glu	Arg	Glu
39-E2H55K181	Ser	His	Glu	Ser	Lys

[a] Viruses were identical with the exception of the indicated positions in the E2 gene.

Infectivity determination by fluorescent center assay. eGFP-expressing double-promoter viruses or replicons were diluted serially in 200 μl PBS–1% DCS, and cell monolayers in 24-well plates were infected for 60 min at 37°C. Monolayers were then washed twice with PBS–1% DCS, overlaid as with the plaque assay, and incubated in growth medium for ~18 h postinfection (hpi). For relative infectivity experiments, BHK cells were infected alongside each other cell line by using an aliquot of the same inoculum. Infectious foci were then quantitated by fluorescence microscopy using a Nikon TE300 microscope with an Endow GFP filter block.

Virus purification. Radiolabeled virus was prepared by infection of BHK cells with stock virus as described previously (24). Virus was labeled with 10 μCi per ml of [^{35}S]methionine and [^{35}S]cysteine (Amersham). Clarified virus preparations were purified on discontinuous 20%–60% sucrose (wt/wt, in TNE buffer [0.05 M Tris hydrochloride {pH 7.2}, 0.1 M NaCl, 0.001 M EDTA]) gradients. For the final concentration, the virus was pelleted through 20% sucrose and resuspended in PBS–1% DCS. The specific infectivity (PFU per counts per minute) of each radiolabeled virus preparation was calculated on BHK cells by a standard plaque assay.

Virus attachment assay. BHK and CHO cells were dissociated from plates using an enzyme-free cell dissociation buffer (Gibco), and binding assays were conducted in suspension. Cells were washed three times with PBS–1% DCS prior to reaction with the virus. For each reaction, 25 μl of cells (~5×10^6) was added to 96-well V-bottom plates (Sarstedt), followed by 25 μl of purified virus (ranging from 5×10^4 to 1×10^5 cpm per reaction), each diluted in different buffers. Reaction mixtures were incubated at 4°C for 60 min with gentle agitation. Cells were then washed three times with 200 μl of diluent, and pellets were resuspended in 100 μl of 0.6% NP-40. Radioactivity associated with cells was enumerated via scintillation counting of 50 μl of the resuspension. Cell-free control reactions were run for each binding experiment, and counts per minute of virus adherent to reaction tubes was subtracted from total counts per minute bound. Binding reactions were done in triplicate, and all experiments were performed at least twice with similar results.

Quantitative PCR titration of virus stocks. We used the SYBR green quantitative PCR (Q-PCR) assay (Bio-Rad) to assess whether or not TR339, 39-E2H55, 39-E2K70, and 39-E2H55K70 mouse inocula contained similar numbers of virus particles (detected as genome equivalents). Briefly, an 80-μl aliquot of each clarified virus stock was digested (20 U; 1 h at 37°C) with RNase One (Promega) to remove contaminating RNA from disrupted cells. Equal volumes of each reaction were subjected to purification using the Ultraspec RNA purification system (Biotecx) with 5 μg of carrier tRNA (Sigma) added to each reaction after the Ultraspec reagent. Equal amounts of purified virus genome-tRNA mixtures were then subjected to reverse transcription (Superscript III polymerase; Invitrogen) using an nsP2-specific primer (5′-CGTGAGGAAGAT TGCGGTTC-3′). Equal volumes of cDNA were then subjected to SYBR green Q-PCR using sets of primers reactive with the nsP2 gene (sense, 5′-CCCAGG AACCCGCAAGTATG-3′; antisense, 5′-TTGTGTGCCCTTCCCAGCTA-3′) downstream of the reverse transcription primer. Q-PCR analysis was completed using a Bio-Rad LightCycler and Bio-Rad Q-PCR analysis software.

In vivo bioluminescence imaging and data quantification. i.c. infection with equal dilutions of 39-REPfLuc, 39-E2H55REPfLuc, 39-E2K70REPfLuc, and 39-E2H55K70REPfLuc replicons or the equivalent fLuc-expressing double-promoter viruses was performed as described above. Before bioluminescence imaging on days 1 and 3 of experiments, the head, abdomen, and back of each animal were shaved to decrease attenuation and scattering of transmitted light by hair. Imaging of firefly luciferase fluorescence in mice was performed on a charge-coupled device camera (Xenogen Corp., Alameda, CA). Briefly, mice were anesthetized by intraperitoneal injection of ketamine-xylazine (90 mg/kg ketamine and 10 mg/kg xylazine). Images were acquired for 2 to 10 s, depending on relative light emission from various sites of infection. Relative intensities of transmitted fluorescence were represented as a pseudocolor image ranging from violet (least intense) to red (most intense). Corresponding gray-scale photographs and color images were superimposed, and relative light intensity was quantitated with LivingImage (Xenogen) image analysis software. Data for four mice per treatment are reported as means ± standard deviations of the means.

Statistical analysis. Statistical significance was determined using a two-tailed Student *t* test with two-sample equal variance.

RESULTS

Construction of viruses. The genotypes of the viruses used in this study are summarized in Table 1. pTR339 is a full-length cDNA clone constructed to encode the consensus sequence of the original wild-type SB AR339 isolate (26, 32; also unpub-

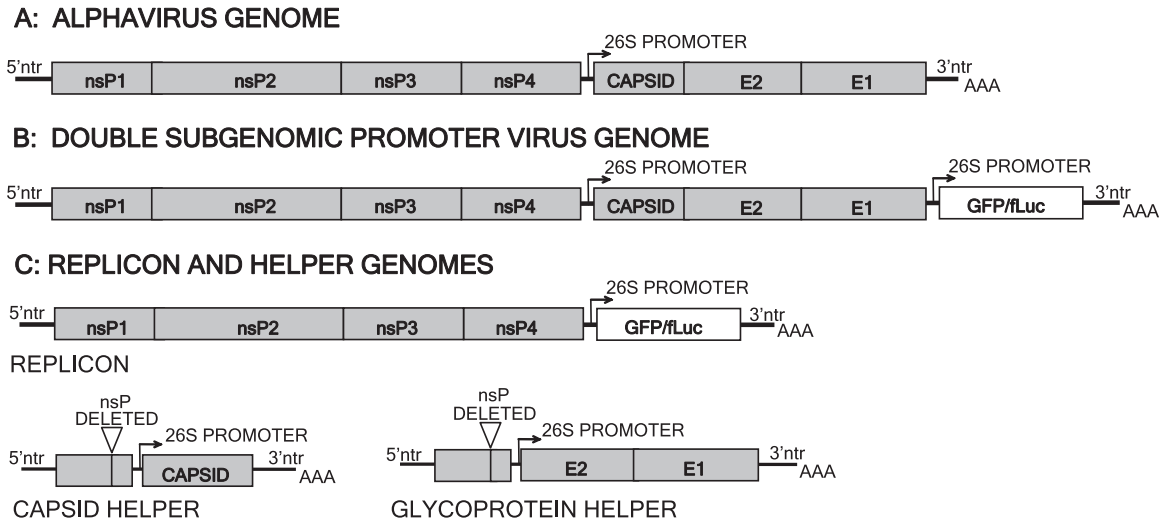

FIG. 1. Diagrams of the genomes of viruses and replicon systems used in the current studies.

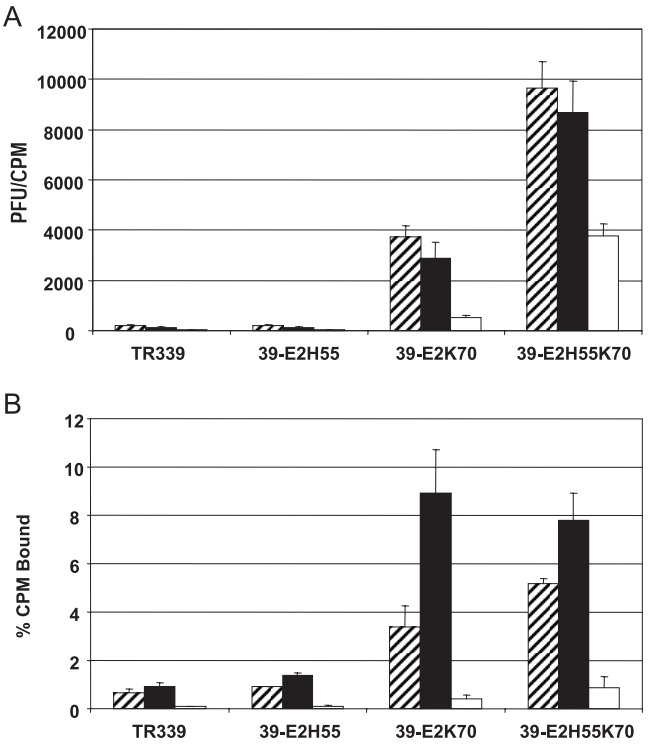

FIG. 2. (A) Differences in BHK cell-specific infectivity (PFU per counts per minute of radiolabeled virus preparations) between TR339, 39-E2H55, 39-E2K70, and 39-E2H55K70 when plaque assay infections were performed in PBS (hatched bars), RPMI (solid bars), or DMEM (open bars) buffer. (B) Attachment of radiolabeled TR339, 39-E2H55, 39-E2K70, or 39-E2H55K70 to BHK cells in PBS (hatched bars), RPMI (solid bars), or DMEM (open bars) buffer. Each reaction mixture received 1×10^5 cpm of purified virus and $\sim 5 \times 10^6$ BHK cells. Data are means of three replicates. Error bars, standard deviations.

lished data) (Fig. 1). The construction of p39-E2K70, containing Lys at E2 position 70 (K70), was also published previously (26). In this study, viruses derived from clones with an E2 His 55 mutation in the pTR339 (p39-E2H55) or p39-E2K70 (p39-E2H55K70) background are compared with pTR339- and p39-E2K70-derived viruses. The p39-E2H55K70 virus was constructed after we passaged virus derived from the p39-E2H55 clone five times in Neuro-2A cell cultures and obtained a mutation from Glu to Lys at E2 70. Viruses in which the E2 His 55 (H55) mutation was placed in the context of other previously identified HS-binding mutations—E2 Arg 1 (R1), E2 Arg 114 (R114) (26), or E2 Lys 181 (K181) (unpublished data)—were also generated. These viruses are designated 39-E2R1H55, 39-E2H55R114, and 39-E2H55K181, respectively. "Double-promoter" viruses expressing eGFP or fLuc from a second subgenomic promoter engineered downstream of the E1 gene were also generated with each E2 mutation(s) (Fig. 1). Nonpropagative SB replicon particles that express eGFP or fLuc have been described elsewhere (36) (Fig. 1).

Relationship of specific infectivity, plaque size, and binding with BHK cells. A recent report indicated that over the pH range of 7.0 to 8.0, the ionic strength of the media or buffers used for attachment assays was important for differences in attachment to N18 neuroblastoma cells between SB strains possessing His versus Gln at E255 (27). The lineage of the viruses in that report indicates that both should possess the K70 mutation and that they differ in E2 only at position 55 (27). In these experiments, the virus with Gln at E2 position 55 exhibited weaker attachment to N18 cells in a medium of higher ionic strength (Dulbecco's modified Eagle medium [DMEM]) and at a pH of 7.0 to 8.0, while attachment to BHK cells was similar for the two viruses under these conditions. The authors concluded that the increased attachment of the His 55-containing virus to the N18 cell line under these conditions was correlated with the greater neurovirulence of SB strains with His at E2 55. We sought to confirm these results, determine their relationship with cell infectivity, and extend them to an evaluation of TR339, 39-E2H55, 39-E2K70, and 39-E2H55K70. We have evaluated the specific infectivity (i.e., the ratio of incorporated counts per minute in purified virus preparations to infectious units), plaque size, and cell binding characteristics of each virus with BHK cells under medium conditions of increasing ionic strength similar to those used by Lee et al. (27): RPMI growth medium buffer (conductivity, 12,777 μS), PBS buffer (conductivity, 13,957 μS), and DMEM growth medium buffer (conductivity, 14,507 μS).

The specific infectivities of TR339, 39-E2H55, 39-E2K70, and 39-E2H55K70 were compared (Fig. 2A). As expected, TR339 exhibited the lowest specific infectivity under all conditions, consistent with the weak cultured-cell attachment exhibited by this virus (26). Introduction of the H55 mutation alone in the TR339 background did not produce a significant change in infectivity for BHK cells ($P > 0.05$ for all buffers). In contrast, introduction of the K70 mutation alone resulted in a substantial increase in infectivity (as much as 20-fold), and the combination of H55 with K70 (39H55K70) resulted in an additional 3- to 8-fold increase in infectivity over that with K70 alone ($P < 0.0001$ for all buffers), depending upon the medium. BHK cell attachment of the radiolabeled viruses was also assessed (Fig. 2B). As with the infectivity results, the presence of K70 resulted in a large increase in attachment, while in the absence of K70, H55 had little effect. The combination of H55 with K70 increased binding slightly over that with K70 alone, but only in the higher-ionic-strength buffers (PBS and DMEM).

Different interactions of virus containing K70 alone versus both H55 and K70 with cultured cells such as BHK were also confirmed by measurement of plaque sizes after infection with the viruses in the three different media (Table 2). Plaque sizes of TR339 and 39-E2H55 were not significantly different when infections were performed in PBS ($P = 0.163$); however, 39-E2H55 plaques were slightly larger in RPMI and DMEM ($P = 0.003$ and 0.009, respectively). The plaques of both viruses

TABLE 2. Plaque sizes of viruses on BHK cells

Virus	Plaque size[a] (mm) of the indicated virus in the following medium:		
	PBS	RPMI	DMEM
TR339	3.0 ± 0.56	3.2 ± 0.50	1.1 ± 0.29
39-E2H55	2.8 ± 0.56	3.7 ± 0.66	1.3 ± 0.40
39-E2K70	4.5 ± 0.75	7.3 ± 1.22	3.5 ± 0.56
39-E2H55K70	5.7 ± 0.86	10.1 ± 1.16	4.5 ± 0.57

[a] Average of 20 plaques.

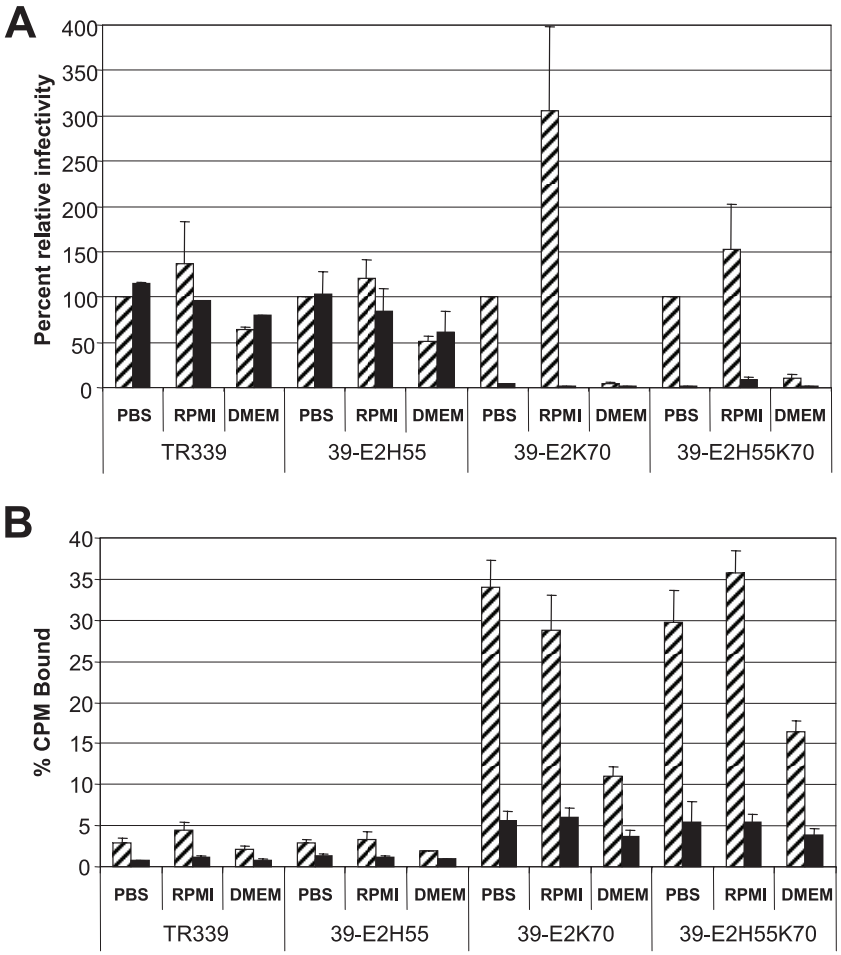

FIG. 3. (A) Relative infectivities of TR339, 39-E2H55, 39-E2K70, and 39-E2H55K70 for CHO K1 control cells (hatched bars) or pgsA745 GAG-deficient cells (solid bars). Infections were performed in either PBS, RPMI, or DMEM buffer. The value for infection of control cells in PBS buffer was set to 100 for each virus, and other infectivities are relative to this value. Wild-type and mutant cells were plated equally in 24-well plates and infected with equal inocula of each eGFP-expressing virus, followed by enumeration of fluorescent cells by microscopy at ~12 h postinfection. (B) Attachment of radiolabeled TR339, 39-E2H55, 39-E2K70, or 39-E2H55K70 to CHO K1 control cells (hatched bars) or pgsA745 GAG-deficient cells (solid bars) in PBS, RPMI, or DMEM buffer. Each reaction mixture received 1×10^5 cpm of purified virus and $\sim 5 \times 10^6$ BHK cells. Data are means of three replicates. Error bars, standard deviations.

were significantly smaller ($P < 0.0001$) than those of 39-E2K70 or 39-E2H55K70, while the plaques of 39-E2H55K70 were significantly larger than those of 39-E2K70 under all conditions ($P < 0.0001$), with the largest difference observed when RPMI (the lowest-ionic-strength medium) was used.

Dependence of binding/infectivity on HS-mediated attachment. In order to determine the effect of the H55 mutation on HS-dependent binding/entry, virus infectivity was evaluated on wild-type CHO K1 cells and CHO mutants defective in GAG synthesis (pgsA-745) (9, 26). Due to variable CPE on these CHO-derived cell lines, double-promoter viruses expressing GFP were used in a fluorescent center assay to evaluate infectivity (Fig. 3A). Consistent with previous results (22), 39-E2K70 virus infected wild-type CHO K1 cells via an HS-dependent mechanism, whereas TR339 virus did not, in PBS or DMEM buffer. 39-E2H55 exhibited infectivity characteristics similar to those of TR339. The infectivity of the 39-E2H55K70 virus exhibited a pattern of dependence on HS similar to that of 39-E2K70; however, the infectivity of 39-E2K70 appeared to be increased to a higher degree in the lowest-ionic-strength buffer. Interestingly, the lowest-ionic-strength buffer, RPMI, increased infection rates for all the viruses, and this increase appeared to be HS dependent in that the additional infectivity was abrogated when the GAG-negative pgsA-745 cells were infected. In contrast, the high-ionic-strength buffer, DMEM, resulted in >90% reductions in the infectivities of 39-E2K70 and 39-E2H55K70 in the presence of HS (wild-type cells) and modest (20 to 40%) reductions in the infectivities of TR339 and 39-E2H55 in either the presence or the absence of HS. Binding to GAG-deficient cells was lower than binding to control cells for all the viruses, and the binding of all viruses to cells expressing HS was lowest in the highest-ionic-strength medium (Fig. 3B). 39-E2K70 and 39-E2H55K70 exhibited similar dependence on the presence of GAG for attachment but bound substantially better than TR339 or 39-E2H55 even in the absence of these structures. We conclude from these studies that 39-E2K70 and 39-E2H55K70 exhibit high dependence (>90% of infecting particles) on HS and that the infectivities

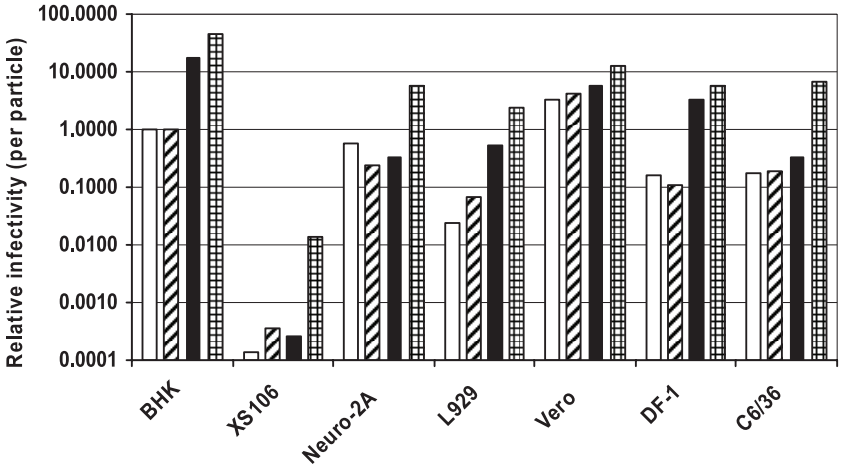

FIG. 4. Relative per-particle infectivity of TR339 (open bars), 39-E2H55 (hatched bars), 39-E2K70 (solid bars), or 39-E2H55K70 (cross-hatched bars) for BHK cells, XS106 mouse dendritic cells (46), Neuro-2A mouse neuroblastoma cells, L929 mouse fibroblast cells, Vero monkey kidney fibroblast cells, DF-1 chicken fibroblast cells, or C6/36 mosquito cells. Infections were performed in PBS using GFP-expressing double subgenomic promoter viruses or replicons. Foci of infection were visualized and counted at 14 to 18 h postinfection using a fluorescence microscope. To determine relative per-particle infectivity, side-by-side infections of BHK cells were completed with each cell line; then the *n*-fold change from BHK cells in infectious units was calculated for each virus-cell line combination and multiplied by the relative specific infectivity (expressed as PFU per counts per minute) of each virus for BHK cells. The infectivity of TR339 (expressed as PFU per counts per minute) for BHK cells was arbitrarily set to 1.0. Data are averages from three separate infections for each cell line.

of both viruses and their binding to HS are sensitive to the ionic strength of DMEM. Furthermore, these results suggest that the infectivity of TR339 (and that of 39-E2H55) is slightly influenced by ionic strength over the ranges tested, with low ionic strength promoting a slight HS-dependent increase in infectivity and high ionic strength promoting a modest inhibition of infectivity independent of HS binding. However, infection by these two viruses was primarily independent of HS interaction, regardless of infection conditions.

Relative infectivity for cultured cells. Lee et al. (27) also recently demonstrated a significant difference between the infectivity of the standard laboratory strain, which possesses Gln at E2 55 (with Lys at E270), and that of a virus containing His at E2 55 (and Lys at 70) for a neuroblastoma cell line (N18) when results were normalized for BHK cell infectivity. Since our results indicated that the H55 mutation increased the BHK cell infectivity for viruses containing K70, we sought to determine if this effect was observed with cell types representative of different mammalian tissues, and also of avian and insect species, by testing the relative infectivity (compared to infectivity for BHK cells) on a panel of cell types (Fig. 4). Our data indicate that the combination of H55 with K70 yielded a virus with the highest infectivity on many different cell types in addition to neuron-like cells, although the highest infectivity was observed with BHK cells.

Effects of mutations on morbidity and mortality of infected mice. Viruses were tested for their abilities to cause morbidity and mortality following s.c. or i.c. inoculation of 6-day-old suckling, 10-day-old suckling, or adult (21-day-old) outbred CD-1 mice (Table 3). Six-day-old and 10-day-old mice were chosen because these ages of mice fall within a period when s.c. inoculation with TR339 is undergoing a rapid transition from uniformly fatal to uniformly nonfatal; this is an interval when virus virulence can be measured with great sensitivity (36). The amount of virus in inocula was normalized by using equal dilutions of virus stocks. As described in the section on specific infectivity above, the mutation of one or two amino acids in E2 can greatly increase the per-particle infectivities of viruses for indicator cells such as BHK. Furthermore, we have determined previously that the 50% lethal dose for TR339 is substantially less than 1 BHK infectious unit (26; also unpublished observations), indicating that particles present in the stocks that can initiate infection in vivo are not enumerated in plaque assays. Therefore, indicator cell infectious units are not an accurate measure of potentially infectious virus particles in a preparation and would lead to great underestimation of the numbers of TR339 particles (for example) in a dose. We have chosen to use equal stock dilutions because (i) stock titers are reproducible over many separate preparations using the different mutants, indicating consistent particle numbers; (ii) purifications of radiolabeled virus particles yield similar amounts (with a maximum difference of two to threefold [data not shown]) for each virus, measured as counts per minute of purified virus particles, suggesting that similar numbers of particles are present in stocks; and (iii) Q-PCR analysis of TR339, 39-E2H55, 39-E2K70, and39-E2H55K70 stocks indicated at most a twofold difference in genome abundance between the viruses (data not shown).

In these experiments we also examined the effects on virulence of several other single-site mutations that, like K70, confer HS binding on TR339. We have previously demonstrated that viruses with a K70, R1, or R114 mutation bind to the cell surface via HS-mediated attachment (23, 26), with the virus containing the R1 mutation exhibiting significantly less efficient binding to HS than the other two. The low affinity of the 39-E2R1 virus binding reflects the partial PE2 cleavage inhibition mechanism through which the R1 mutation confers HS binding (23). The K181 mutation was selected by passage of TR339 on differentiated C2C12 murine skeletal muscle cells. The infectivity of the 39-E2K181 virus was reduced >90% on

TABLE 3. Mortality rates and average survival times of CD-1 mice of various ages infected with different SB E2 mutants[a]

Type of inoculation and virus	Result for mice of the following age at infection:					
	6 days[b]		10 days[c]		21 days[d]	
	% Mortality	AST (days)	% Mortality	AST (days)	% Mortality	AST (days)
Subcutaneous						
TR339	100	6.1 ± 1.0	ND[e]		0	
39-E2H55	100	6.8 ± 1.3	ND		0	
39-E2K70	85.7	8.3 ± 1.9	ND		0	
39-E2H55K70	100	1.5 ± 0.4	ND		100	7.0 ± 0.7
39-E2R1	41.7	9.1 ± 1.7	ND		0	
39-E2R114	83.3	10.5 ± 1.4	ND		0	
39-E2K181	50	9.3 ± 1.4	ND		0	
39-E2H55R1	ND		ND		0	
39-E2H55R114	ND		ND		0	
39-E2H55K181	ND		ND		0	
Intracranial						
TR339	100	6.0 ± 1.0	83.3	6.7 ± 2.4	0	
39-E2H55	100	5.8 ± 1.3	81.8	6.3 ± 1.2	0	
39-E2K70	100	3.9 ± 1.0	100	4.8 ± 0.9	0	
39-E2H55K70	100	2.3 ± 0.5	100	2.8 ± 0.4	100	6.2 ± 0.8
39-E2R1	100	6.4 ± 1.4	63.6	6.4 ± 2.0	0	
39-E2R114	100	5.9 ± 2.0	100	5.1 ± 0.9	0	
39-E2K181	100	4.7 ± 0.9	81.8	4.8 ± 0.8	0	
39-E2H55R1	ND		45.4	7.0 ± 2.0	0	
39-E2H55R114	ND		45.4	8.8 ± 1.3	0	
39-E2H55K181	ND		81.8	6.1 ± 1.7	0	

[a] Mice were infected with equal dilutions of each stock of virus as described in Materials and Methods. Each experiment was performed at least twice with similar results.
[b] Each group contained 21 to 24 mice.
[c] Each group contained 10 mice.
[d] Each group contained 5 mice.
[e] ND, not determined.

HS-deficient pgsA-745 CHO cells, demonstrating the HS dependence of infection by this virus (data not shown).

As expected, all of the HS-binding single-site mutants were attenuated in comparison with TR339 after s.c. inoculation of 6-day-old mice (Table 3). Surprisingly, however, several HS-binding mutations increased virulence over that of TR339 when viruses were delivered i.c. to mice of this age; AST for mice infected with the 39-E2K70 and 39-E2K181 viruses shortened significantly ($P < 0.001$ and $P = 0.001$, respectively). For mice infected i.c. at the age of 10 days, TR339 and 39-E2H55 were not uniformly lethal, while 39-E2K70 and 39-E2R114 were, and the 39-E2K70 and 39-E2K181 viruses produced significantly reduced AST ($P = 0.02$ and $P = 0.03$, respectively). In these experiments, the 39-E2R1 HS-binding mutation failed to decrease AST or increase mortality versus that with TR339. This mutation, adjacent to the furin protease cleavage site of PE2, functions to increase HS binding by decreasing the efficiency of PE2 cleavage, resulting in retention of the positively charged furin protease cleavage/HS-binding sequence (23). This is in contrast with the K70, R114, or K181 mutation, which does not alter this phenotype (23; also data not shown). Since retention of PE2 is attenuating at least in part due to the inhibition of virus fusion processes (38), it is possible that effects of HS binding on virulence may be masked by unrelated attenuating characteristics of PE2-containing viruses. Notably, the H55 mutation alone had little effect on TR339 mortality or AST regardless of the route or the age of the mouse inoculated ($P = 0.060$ for 6-day-old mice inoculated s.c; $P = 0.651$ for 6-day-old mice inoculated i.c.; $P = 0.681$ for 10-day-old mice inoculated i.c.), and no single mutation was capable of causing fatal disease in a 21-day-old mouse. However, when the H55 mutation was combined with the HS-binding mutation K70, 100% mortality was observed in 21-day-old mice from both the s.c. and i.c. routes. The 39-E2H55K70 virus was also capable of causing 100% mortality when inoculated i.c. into 5-week-old mice; however, no mortality resulted from an s.c. inoculation of mice of this age (data not shown). These results indicate that H55 and K70 are both required to confer adult mouse virulence on TR339. Furthermore, these results suggest that HS binding may contribute directly to virus virulence when the requirements for viremic spread are eliminated. Interestingly, the 39-E2H55K70 virus was more virulent than TR339 under all circumstances tested, regardless of the infection route, and even reduced AST in comparison with TR339 for 1-day-old mice regardless of the inoculation route (data not shown).

Virus replication in brains of i.c. inoculated 10-day-old CD-1 mice. To examine whether or not quantitative aspects of virus replication in vivo were related to the virulence differences between viruses with polymorphisms at E2 55 or E2 70, we compared the replication of TR339, 39-E2H55, 39-E2K70, and 39-E2H55K70 in i.c. infected 10-day-old mice, since for mice this age reveals significant differences in mortality and AST between TR339, 39-E2K70, and 39-E2H55K70 (Table 3). Attempts to titer virus from serum and brains were complicated by the differences in BHK cell infectivity between the virus strains. Therefore, we utilized firefly luciferase-expressing

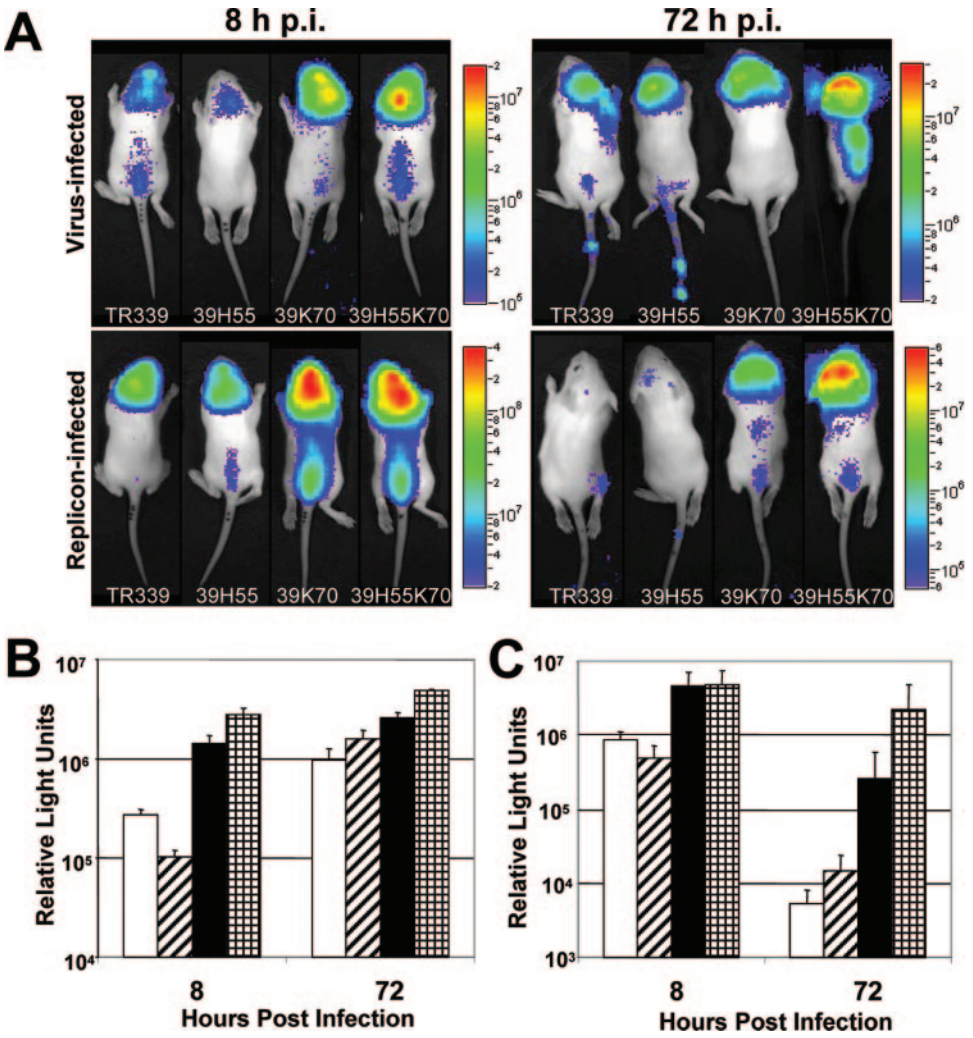

FIG. 5. In vivo imaging of 10-day-old mice at 8 or 72 h after infection (p.i.) with luciferase-expressing viruses (A and B) or replicons (A and C). Groups of four mice were inoculated with 10 μl of equal dilutions of each stock (equivalent to 10^4 PFU of TR339). Mice were imaged for 2 to 10 s to prevent image saturation. (A) Observable image of one representative mouse from each group. (B) Quantitation (Living Image software; Xenogen) of relative light units emitted from the heads of mice infected with TR339 (open bars), 39-E2H55 (hatched bars), 39-E2K70 (solid bars), or 39-E2H55K70 (cross-hatched bars) virus. (C) Quantitation of relative light units emitted from the heads of mice infected with analogous replicons. Data are averages of relative light units emitted from four mice. Error bars, standard deviations.

double subgenomic promoter viruses and nonpropagative replicons with Xenogen In vivo Imaging System (IVIS) bioluminescence analysis to examine virus replication. IVIS was used previously to examine Sindbis strain NSV replication in mice (6). In these studies, emitted light was found to correlate well with virus replication as calculated from titration of PFU from infected tissues.

At 8 hpi, the 39-E2K70 and 39-E2H55K70 viruses and replicons exhibited 5- to10-fold-higher levels of replication than TR339 or 39-E2H55 as measured by IVIS (Fig. 5A, B, and C). Replication of all viruses increased between 8 and 72 hpi, with the TR339 and 39-E2H55 viruses showing larger increases in the signal over this interval than 39-E2K70 or 39-E2H55K70, although ultimately the non-HS-binding viruses produced less total luciferase signal (Fig. 5A and B). With the replicons, all signals decreased between 8 and 72 hpi, as expected, but there was a dramatic difference between E2 proteins in the clearance of replication, with TR339, 39-E2H55, and 39-E2K70 exhibiting ~20- to 150-fold reductions in luminescence, while luminescence for 39-E2H55K70 was only ~2-fold lower (Fig. 5A and C).

Virulence of His 55 in combination with other HS-binding mutations. In these experiments, we sought to determine if the effect of the K70 HS-binding mutation on the virulence of 39-E2H55K70 was due solely to promiscuous HS interaction, possibly through a simple increase in cell binding by viruses allowing increased H55-mediated activity. If this were the case, we would expect the combination of other HS-binding mutations to have an effect similar to that of K70 on the virulence of H55-containing viruses. However, infection of mice with viruses combining the H55 mutation with R1, K181, or R114, each of which confers HS binding when introduced into TR339 (23, 26; also these studies), did not yield viruses capable of causing mortality in adult mice (Table 3). In fact, several of

these viruses were less virulent in all of our models than TR339 (Table 3 and data not shown). Therefore, the adult neurovirulence of 39-E2H55K70 is attributable to an unidentified aspect of this particular combination of amino acids and is not due to separate effects of increased HS-dependent cell binding and H55-mediated activities.

DISCUSSION

Infection with the consensus wild-type strain TR339 causes fatal disease in suckling mice but not in weanling mice (36). This is also true of laboratory strains of SB, such as the SV strain, that have been adapted to growth in cell culture (15, 22), although these viruses are more attenuated, causing the transition from fatal to nonfatal infection to occur at an earlier age (36). The exception is NSV, a neuroadapted variant of the SV laboratory strain that elicits severe, often fatal encephalomyelitis in adult mice (17). NSV appears to target the same types of neurons as SV but interacts with cells in a manner that produces more-severe encephalomyelitis (17, 27). We have demonstrated that this phenotype is dependent on the combination of H55 and K70 mutations and is very likely associated with HS binding. Furthermore, single-site mutations in E2 that confer HS binding to TR339 can also increase the virulence of the virus when delivered i.c. Whether or not adult neurovirulence of 39-E2H55K70 is directly due to HS-mediated attachment in vivo cannot be confirmed, because the other HS-binding mutations coupled with E2 His 55 do not enhance disease.

The K70 mutation is common to a number of SB laboratory strains (32) and was likely present in the original SB strain utilized by Griffin and coworkers to select for the H55 mutation (17). We have previously selected the K70 mutation by passaging TR339 in several fibroblast cell types, including mammalian BHK, CHO, and Vero cells and avian DF-1 cells (data not shown). In the current studies, we selected for the K70 mutation by passaging 39-E2H55 in neuro-2A murine neuroblastoma cells. However, passaging of TR339 in these cells resulted in the acquisition of different mutations (data not shown). Therefore, we cannot say definitively whether or not there is coselection in vitro for the H55 and K70 mutations in the TR339 background.

Our results generally confirm the studies of Lee et al. (27) with respect to the influence of ionic strength on the cell attachment phenotype of SB with K70 and H55 and extend these results to examine the effects, individually, of each of these mutations in the background of the consensus wild-type AR339 strain. However, in contrast with the previous study, differences in infectivity between standard SB laboratory strains (represented by 39-E2K70) and viruses containing H55 and K70 were detected with all cultured cell types examined, not just neural tissue-derived cells. However, it should be noted that increased BHK cell replication of an SB strain containing His versus Gln at E2 position 55 has been reported previously (42). While differences exist between clones derived from TR339 and the Sindbis virus 633 and TE isolates utilized by these other investigators in the 5′ and 3′ nontranslated regions and the nsPs and E1 genes, the E2 genes of the 633 and TE viruses should be the same as that of TR339 outside of the 55/70 loci (29, 32). Whether or not genetic variation in E1 or in other regions of the genome accounts for the differences between our results and those of Lee et al. (27) remains to be determined. Nevertheless, our results indicate that the combination of H55 with K70 can confer a uniquely high degree of infectivity on the consensus sequence SB that is evident during infection of many cell types.

A comparison of specific infectivity and cell attachment data suggests that the increase in the infectivity of 39-E2K70 versus TR339 is due primarily to an increase in HS-mediated attachment to cells. The increase in the infectivity of 39-E3H55K70 compared with that of 39-E2K70 (three- to fivefold depending upon the buffer) is not consistently reflected in an increase in binding. Furthermore, the H55 mutation alone has no discernible effect on TR339 binding, infectivity, or virulence. Therefore, we conclude that, at least with respect to the cell types tested, when in combination with K70, the H55 mutation appears to increase cell infectivity independently of consistent measurable effects on initial HS binding. The combination of H55 with K70 may increase the efficiency of post-HS-binding events in the infection pathway; possibly by promoting fusion of HS-bound viruses, enhancing or altering interactions with a primary receptor, or redirecting the entering virion to a coreceptor structure. Furthermore, this effect is specific to this specific combination of mutations and is not a function of promiscuous HS attachment.

It will be important to determine if the enhanced adult mouse virulence of the 39-E2H55K70 virus or of viruses containing single E2-positive charge mutations is simply a function of enhanced numbers of infected brain cells, as recently proposed for the NSV strain by Lee et al. (27), or if the altered interaction of these viruses with cell surface structures promotes postentry events associated with SB neuropathogenesis. In mice, viruses containing individual HS-binding mutations were attenuated from the s.c. route in comparison with TR339, while 39-E2H55K70 was uniformly more virulent than TR339 regardless of the route. Whether or not this difference is accounted for by increased infectivity alone is not certain. Our IVIS studies indicated that the initial replication of 39-E2K70 and the initial replication of 39-E2H55K70 in the brains of 10-day-old mice were similarly higher than those of the non-HS-binding viruses; however, the replication of 39-H55K70 diminished in infected cells much more slowly than those of either the non-HS-binding or HS-binding strains with single mutations. This also suggests a postattachment effect of the H55–K70 combination, allowing prolonged virus protein expression in infected cells. Recent studies have indicated that the 67-kDa high-affinity laminin receptor (HALR), the cell surface receptor identified for presumably HS-binding SB laboratory strains (45), is an HS-binding (12, 20) cell surface signaling molecule. Ligand interaction with this receptor can affect mitogen-activated kinase phosphorylation (13) and cytoskeleton remodeling (10, 11). Therefore, it is possible that an altered interaction of 39-E2H55K70 with the HS-containing HALR complex could also have a qualitative effect on the fates of infected cells and mouse pathogenesis. It is becoming increasingly apparent that subtle differences in the configuration, carbohydrate structure, or charge of the virion's spike proteins may dramatically alter the virulence and apparent tropisms of alphaviruses. We have recently demonstrated a similar phenomenon in the C-type lectin receptor usage of mosquito cell-

derived versus mammalian-cell-derived SB. We have tested the DC-SIGN and L-SIGN C-type lectin specificities of 39-E2H55 and 39-E2H55K70, but they are not altered compared with that of TR339 (data not shown).

These results promote the idea that HS-binding mutants with increased cell infectivities could arise during the replication cycle of an alphavirus within a single vertebrate host, perhaps exacerbating damage to particular tissues later in infection. HS binding contributes to the severity of encephalitis after infection with Theiler's murine encephalomyelitis virus (35). The fact that RNA viruses exist as rapidly adaptable quasispecies (7) makes this idea even more appealing. We would further speculate that mutations may arise that confer interaction with specific HS structures present in different tissues. We have found that different HS-binding mutations can be obtained by passage of TR339 in cells derived from different tissue types in vitro (e.g., K181 [this work]) (unpublished results).

Together, our studies and the work of others (1, 5, 18, 26, 39) suggest that efficient HS binding is inhibitory to the magnitude and duration of viremia and can lead to attenuation of viruses that are delivered through the skin and thus require systemic dissemination or transit to the CNS in order to elicit disease. However, our new evidence suggests that it is also possible that particular viruses may have either very high infectivity or a receptor interaction that alters postbinding events (e.g., 39-E2H55K70) such that the effects of promiscuous cell binding are overcome provided some virus particles reach the brain. Whether or not these viruses would attain sufficient viremia for transmission to arthropod vectors and spread between vertebrate hosts remains to be determined. However, these results suggest that HS binding could be a component of the replication cycle of alphaviruses circulating in nature. Of particular interest may be alphaviruses, such as EEEV, that cause very high rates of mortality in humans and equines due to replication in the CNS. Definitive study of this possibility will require the resurrection of E2 proteins directly from mosquitoes or vertebrates infected naturally, due to the potential for artifactual HS binding acquired by alphaviruses during isolation.

ACKNOWLEDGMENTS

These studies were supported by NIH grant R01 AI22186-19.

Janice Anderson, Tanya Debenport, Paul Schuetze, and Michael Farmer provided excellent technical assistance.

REFERENCES

1. **Bernard, K. A., W. B. Klimstra, and R. E. Johnston.** 2000. Mutations in the E2 glycoprotein of Venezuelan equine encephalitis virus confer heparan sulfate interaction, low morbidity, and rapid clearance from blood of mice. Virology **276:**93–103.
2. **Bredenbeek, P. J., I. Frolov, C. M. Rice, and S. Schlesinger.** 1993. Sindbis virus expression vectors: packaging of RNA replicons by using defective helper RNAs. J. Virol. **67:**6439–6446.
3. **Burgess, T. H., K. E. Steele, B. A. Schoneboom, and F. B. Grieder.** 2001. Clinicopathologic features of viral agents of potential use by bioterrorists. Clin. Lab. Med. **21:**475–493, viii.
4. **Byrnes, A. P., and D. E. Griffin.** 1998. Binding of Sindbis virus to cell surface heparan sulfate. J. Virol. **72:**7349–7356.
5. **Byrnes, A. P., and D. E. Griffin.** 2000. Large-plaque mutants of Sindbis virus show reduced binding to heparan sulfate, heightened viremia, and slower clearance from the circulation. J. Virol. **74:**644–651.
6. **Cook, S. H., and D. E. Griffin.** 2003. Luciferase imaging of a neurotropic viral infection in intact animals. J. Virol. **77:**5333–5338.
7. **Domingo, E., E. Martinez-Salas, F. Sobrino, J. C. de la Torre, A. Portela, J. Ortin, C. Lopez-Galindez, P. Perez-Brena, N. Villanueva, R. Najera, et al.** 1985. The quasispecies (extremely heterogeneous) nature of viral RNA genome populations: biological relevance—a review. Gene **40:**1–8.
8. **Dropulic, L. K., J. M. Hardwick, and D. E. Griffin.** 1997. A single amino acid change in the E2 glycoprotein of Sindbis virus confers neurovirulence by altering an early step of virus replication. J. Virol. **71:**6100–6105.
9. **Esko, J. D., T. E. Stewart, and W. H. Taylor.** 1985. Animal cell mutants defective in glycosaminoglycan biosynthesis. Proc. Natl. Acad. Sci. USA **82:**3197–3201.
10. **Fujimura, Y., D. Umeda, Y. Kiyohara, Y. Sunada, K. Yamada, and H. Tachibana.** 2006. The involvement of the 67 kDa laminin receptor-mediated modulation of cytoskeleton in the degranulation inhibition induced by epigallocatechin-3-*O*-gallate. Biochem. Biophys. Res. Commun. **348:**524–531.
11. **Fujimura, Y., K. Yamada, and H. Tachibana.** 2005. A lipid raft-associated 67-kDa laminin receptor mediates suppressive effect of epigallocatechin-3-*O*-gallate on FεRI expression. Biochem. Biophys. Res. Commun. **336:**674–681.
12. **Gauczynski, S., D. Nikles, S. El Gogo, D. Papy-Garcia, C. Rey, S. Alban, D. Barritault, C. I. Lasmezas, and S. Weiss.** 2006. The 37-kDa/67-kDa laminin receptor acts as a receptor for infectious prions and is inhibited by polysulfated glycanes. J. Infect. Dis. **194:**702–709.
13. **Givant-Horwitz, V., B. Davidson, and R. Reich.** 2004. Laminin-induced signaling in tumor cells: the role of the M_r 67,000 laminin receptor. Cancer Res. **64:**3572–3579.
14. **Goodfellow, I. G., A. B. Sioofy, R. M. Powell, and D. J. Evans.** 2001. Echoviruses bind heparan sulfate at the cell surface. J. Virol. **75:**4918–4921.
15. **Griffin, D. E.** 1976. Role of the immune response in age-dependent resistance of mice to encephalitis due to Sindbis virus. J. Infect. Dis. **133:**456–464.
16. **Griffin, D. E.** 2001. Alphaviruses, p. 917–962. *In* D. M. Knipe, P. M. Howley, D. E. Griffin, R. A. Lamb, M. A. Martin, B. Roizman, and S. E. Straus (ed.), Fields virology. Lippincott Williams & Wilkins, Philadelphia, Pa.
17. **Griffin, D. E., and R. T. Johnson.** 1977. Role of the immune response in recovery from Sindbis virus encephalitis in mice. J. Immunol. **118:**1070–1075.
18. **Heil, M. L., A. Albee, J. H. Strauss, and R. J. Kuhn.** 2001. An amino acid substitution in the coding region of the E2 glycoprotein adapts Ross River virus to utilize heparan sulfate as an attachment moiety. J. Virol. **75:**6303–6309.
19. **Hulst, M. M., H. G. van Gennip, and R. J. Moormann.** 2000. Passage of classical swine fever virus in cultured swine kidney cells selects virus variants that bind to heparan sulfate due to a single amino acid change in envelope protein E^{rns}. J. Virol. **74:**9553–9561.
20. **Hundt, C., J. M. Peyrin, S. Haik, S. Gauczynski, C. Leucht, R. Rieger, M. L. Riley, J. P. Deslys, D. Dormont, C. I. Lasmezas, and S. Weiss.** 2001. Identification of interaction domains of the prion protein with its 37-kDa/67-kDa laminin receptor. EMBO J. **20:**5876–5886.
21. **Jan, J. T., and D. E. Griffin.** 1999. Induction of apoptosis by Sindbis virus occurs at cell entry and does not require virus replication. J. Virol. **73:**10296–10302.
22. **Johnson, R. T., H. F. McFarland, and S. E. Levy.** 1972. Age-dependent resistance to viral encephalitis: studies of infections due to Sindbis virus in mice. J. Infect. Dis. **125:**257–262.
23. **Klimstra, W. B., H. W. Heidner, and R. E. Johnston.** 1999. The furin protease cleavage recognition sequence of Sindbis virus PE2 can mediate virion attachment to cell surface heparan sulfate. J. Virol. **73:**6299–6306.
24. **Klimstra, W. B., E. M. Nangle, M. S. Smith, A. D. Yurochko, and K. D. Ryman.** 2003. DC-SIGN and L-SIGN can act as attachment receptors for alphaviruses and distinguish between mosquito cell- and mammalian cell-derived viruses. J. Virol. **77:**12022–12032.
25. **Klimstra, W. B., K. D. Ryman, K. A. Bernard, K. B. Nguyen, C. A. Biron, and R. E. Johnston.** 1999. Infection of neonatal mice with Sindbis virus results in a systemic inflammatory response syndrome. J. Virol. **73:**10387–10398.
26. **Klimstra, W. B., K. D. Ryman, and R. E. Johnston.** 1998. Adaptation of Sindbis virus to BHK cells selects for use of heparan sulfate as an attachment receptor. J. Virol. **72:**7357–7366.
27. **Lee, P., R. Knight, J. M. Smit, J. Wilschut, and D. E. Griffin.** 2002. A single mutation in the E2 glycoprotein important for neurovirulence influences binding of Sindbis virus to neuroblastoma cells. J. Virol. **76:**6302–6310.
28. **Lewis, J., S. L. Wesselingh, D. E. Griffin, and J. M. Hardwick.** 1996. Alphavirus-induced apoptosis in mouse brains correlates with neurovirulence. J. Virol. **70:**1828–1835.
29. **Lustig, S., A. C. Jackson, C. S. Hahn, D. E. Griffin, E. G. Strauss, and J. H. Strauss.** 1988. Molecular basis of Sindbis virus neurovirulence in mice. J. Virol. **62:**2329–2336.
30. **MacDonald, G. H., and R. E. Johnston.** 2000. Role of dendritic cell targeting in Venezuelan equine encephalitis virus pathogenesis. J. Virol. **74:**914–922.
31. **Mandl, C. W., H. Kroschewski, S. L. Allison, R. Kofler, H. Holzmann, T. Meixner, and F. X. Heinz.** 2001. Adaptation of tick-borne encephalitis virus to BHK-21 cells results in the formation of multiple heparan sulfate binding sites in the envelope protein and attenuation in vivo. J. Virol. **75:**5627–5637.
32. **McKnight, K. L., D. A. Simpson, S. C. Lin, T. A. Knott, J. M. Polo, D. F. Pence, D. B. Johannsen, H. W. Heidner, N. L. Davis, and R. E. Johnston.** 1996. Deduced consensus sequence of Sindbis virus strain AR339: mutations

contained in laboratory strains which affect cell culture and in vivo phenotypes. J. Virol. **70:**1981–1989.
33. **Nargi-Aizenman, J. L., M. B. Havert, M. Zhang, D. N. Irani, J. D. Rothstein, and D. E. Griffin.** 2004. Glutamate receptor antagonists protect from virus-induced neural degeneration. Ann. Neurol. **55:**541–549.
34. **Neff, S., D. Sa-Carvalho, E. Rieder, P. W. Mason, S. D. Blystone, E. J. Brown, and B. Baxt.** 1998. Foot-and-mouth disease virus virulent for cattle utilizes the integrin $\alpha_v\beta_3$ as its receptor. J. Virol. **72:**3587–3594.
35. **Reddi, H. V., A. S. Kumar, A. Y. Kung, P. D. Kallio, B. P. Schlitt, and H. L. Lipton.** 2004. Heparan sulfate-independent infection attenuates high-neurovirulence GDVII virus-induced encephalitis. J. Virol. **78:**8909–8916.
36. **Ryman, K. D., C. L. Gardner, K. C. Meier, C. A. Biron, R. E. Johnston, and W. B. Klimstra.** 2007. Early restriction of alphavirus replication and dissemination contributes to age-dependent attenuation of systemic hyperinflammatory disease. J. Gen. Virol. **88:**518–529.
37. **Ryman, K. D., L. J. White, R. E. Johnston, and W. B. Klimstra.** 2002. Effects of PKR/RNase L-dependent and alternative antiviral pathways on alphavirus replication and pathogenesis. Viral Immunol. **15:**53–76.
38. **Smit, J. M., W. B. Klimstra, K. D. Ryman, R. Bittman, R. E. Johnston, and J. Wilschut.** 2001. PE2 cleavage mutants of Sindbis virus: correlation between viral infectivity and pH-dependent membrane fusion activation of the spike heterodimer. J. Virol. **75:**11196–11204.
39. **Smit, J. M., B. L. Waarts, K. Kimata, W. B. Klimstra, R. Bittman, and J. Wilschut.** 2002. Adaptation of alphaviruses to heparan sulfate: interaction of Sindbis and Semliki forest viruses with liposomes containing lipid-conjugated heparin. J. Virol. **76:**10128–10137.
40. **Trgovcich, J., J. F. Aronson, J. C. Eldridge, and R. E. Johnston.** 1999. TNFα, interferon, and stress response induction as a function of age-related susceptibility to fatal Sindbis virus infection of mice. Virology **263:**339–348.
41. **Trybala, E., A. Roth, M. Johansson, J. A. Liljeqvist, E. Rekabdar, O. Larm, and T. Bergstrom.** 2002. Glycosaminoglycan-binding ability is a feature of wild-type strains of herpes simplex virus type 1. Virology **302:**413–419.
42. **Tucker, P. C., E. G. Strauss, R. J. Kuhn, J. H. Strauss, and D. E. Griffin.** 1993. Viral determinants of age-dependent virulence of Sindbis virus for mice. J. Virol. **67:**4605–4610.
43. **Ubol, S., P. C. Tucker, D. E. Griffin, and J. M. Hardwick.** 1994. Neurovirulent strains of Alphavirus induce apoptosis in bcl-2-expressing cells: role of a single amino acid change in the E2 glycoprotein. Proc. Natl. Acad. Sci. USA **91:**5202–5206.
44. **Vogel, P., D. L. Fritz, K. Kuehl, K. J. Davis, and T. Geisbert.** 1997. The agents of biological warfare. JAMA **278:**438–439.
45. **Wang, K. S., R. J. Kuhn, E. G. Strauss, S. Ou, and J. H. Strauss.** 1992. High-affinity laminin receptor is a receptor for Sindbis virus in mammalian cells. J. Virol. **66:**4992–5001.
46. **Xu, S., K. Ariizumi, D. Edelbaum, P. R. Bergstresser, and A. Takashima.** 1995. Cytokine-dependent regulation of growth and maturation in murine epidermal dendritic cell lines. Eur. J. Immunol. **25:**1018–1024.